Supporting Information

Ishitani *et al.* 10.1073/pnas.0802991105

SI Text

SI Results and Discussion: Protease Protection Assay. We performed the protease protection assay to probe the structural changes depending on the divalent cation concentration. The results showed that MgtE is highly susceptible to proteolysis without Mg^{2+}, whereas it is partly protected from proteolysis with ≈10 mM Mg^{2+} (Fig. S7*A*). The N-terminal sequencing of these proteolytic fragments revealed that the protease-resistant fragment that appeared at the highest Mg^{2+} concentration starts from residue 129 and lacks the N domain. Moreover, its molecular weight approximated from the electrophoretic mobility, suggested that the fragment contains all of the CBS and TM domains. Therefore, under the conditions of 32 mM Mg^{2+}, it is likely that only the CBS domain was in the closed form, or both the N and CBS domains were in the closed form, but the loop between the N and CBS domains was flexible and susceptible to proteolysis. In either case, these results suggest that the Mg^{2+}-dependent structural change of the CBS domain actually occurs in solution and that its K_d value is in the millimolar range, which seems to be feasible, considering the physiological concentration of cytosolic Mg^{2+} (1). Furthermore, the results showed that MgtE is also weakly protected from proteolysis with Ca^{2+} in the millimolar range (Fig. S7*B*). The Ca^{2+} ions may also bind to MgtE and stabilize the closed-form structure, supporting the observation in the Ca5 simulations.

SI Methods. ***Modeling of initial structures.*** The initial structures of the closed-to-open form simulations (i.e., C456, C0, C5, and C46) were built from the crystal structure of the Mg^{2+}-bound MgtE cytosolic domains from *Thermus thermophilus* (PDB ID code 2YVY) (2). The Mg^{2+} binding sites investigated in the present simulations (Mg4, Mg5, and Mg6) were selected by carefully examining the crystal structure of the cytosolic domain, as well as that from another organism (PDB ID code 2OUX) and the full-length structure of MgtE (PDB ID code 2YVX). As for Mg5, the coordinated water molecules, which were not observed in the crystal structure, were modeled to form the standard octahedral geometry. All of the water molecules observed in the crystal structure were kept. Especially, the water molecules coordinated to Mg4 and Mg6 are observed in the crystal structure, and therefore these coordinates were used as the initial structure. Hydrogen atoms were added by using the PSFGEN plugin of VMD (3). The system was then solvated to form a 108 × 108 × 108-Å cubic simulation box by using the Solvate plugin of VMD. The resulting solvated system was neutralized by randomly adding Na^+ ions in the bulk water.

The initial structure of the O5 simulation was built from the snapshot at 20 ns of the C0 simulation (C0F) by simply removing the N domains and adding Mg^{2+} at site 5. The water molecules coordinated to these Mg^{2+} ions were modeled to form the standard octahedral geometry. In addition, water molecules ≈5 Å from the protein in the same snapshot, with positions that did not clash with the modeled ions and water molecules, were also kept. The system was then solvated to form a 90 × 90 × 90-Å cubic simulation box and was neutralized by Na^+.

For the O465 simulation, we had to model the initial structure, in which the conformation of the N and CBS domains is in the closed form, whereas the intersubunit orientation between the CBS domains is in the same open form as the O5 simulation. For this purpose, we modeled the initial structure by replacing the open-form N domains of C0F, which was also used as the initial structure of the O5 simulation, with those in the closed form. As the N domains in the closed form, we used the snapshot structure of the C456 simulation at 5 ns (C456I). The detailed procedure is as follows. At first, the protein and Mg^{2+} coordinates of the A subunit of C465I were superimposed on those of C0F by fitting the Cα atoms of the CBS domain (132–245) by the least-squares method. The rmsd value for the CBS domains was 1.4 Å, indicating that the CBS domains of C0F and C465I had almost the same structures. Then we replaced the open-form N domain (1–131) in C0F with the closed-form N domain in C465. In this step we also replaced the CBS2 domain (204–245) including Mg4 and Mg6 to avoid steric clashes between the N and CBS2 domains and to keep the proper protein–Mg^{2+} interactions at sites 4 and 6. On the other hand, to avoid steric clashes of the side chains at the intersubunit interface, the coordinates of the CBS1 domain (132–203) were kept as in C0F. Mg5 and its coordinated water molecules were built by the same method as in the O5 simulation described above. The structure of chain B was also built in the same manner. The system was then solvated to form a 108 × 108 × 108-Å cubic simulation box and was neutralized by Na^+.

Limited proteolysis assay. The full-length MgtE protein was prepared as described (4). For the 10-μl reaction volumes, stock solutions were prepared to produce the final concentrations desired upon dilution: 8 μl of full-length MgtE (1.06 mg/ml), 1 μl of trypsin (15.6 μg/ml; Sigma), and 1 μl of 0–32 mM divalent cation (Mg^{2+} or Ca^{2+}). Reaction solutions were mixed and equilibrated at 4°C for 30–40 min. Trypsin was then added, and reactions were incubated at 4°C for 17 h. After adding 10 μl of SDS/PAGE sample buffer, the samples were boiled and run immediately on 12.5% SDS/PAGE gels.

1. Maguire ME, Cowan JA (2002) Magnesium chemistry and biochemistry. *Biometals* 15:203–210.
2. Hattori M, Tanaka Y, Fukai S, Ishitani R, Nureki O (2007) Crystal structure of the MgtE Mg2+ transporter. *Nature* 448:1072–1075.
3. Humphrey W, Dalke A, Schulten K (1996) VMD: Visual molecular dynamics. *J Mol Graphics* 14:33–38.
4. Hattori M, Tanaka Y, Fukai S, Ishitani R, Nureki O (2007) Crystallization and preliminary x-ray diffraction analysis of the full-length Mg^{2+} transporter MgtE. *Acta Crystallogr F* 63:682–684.

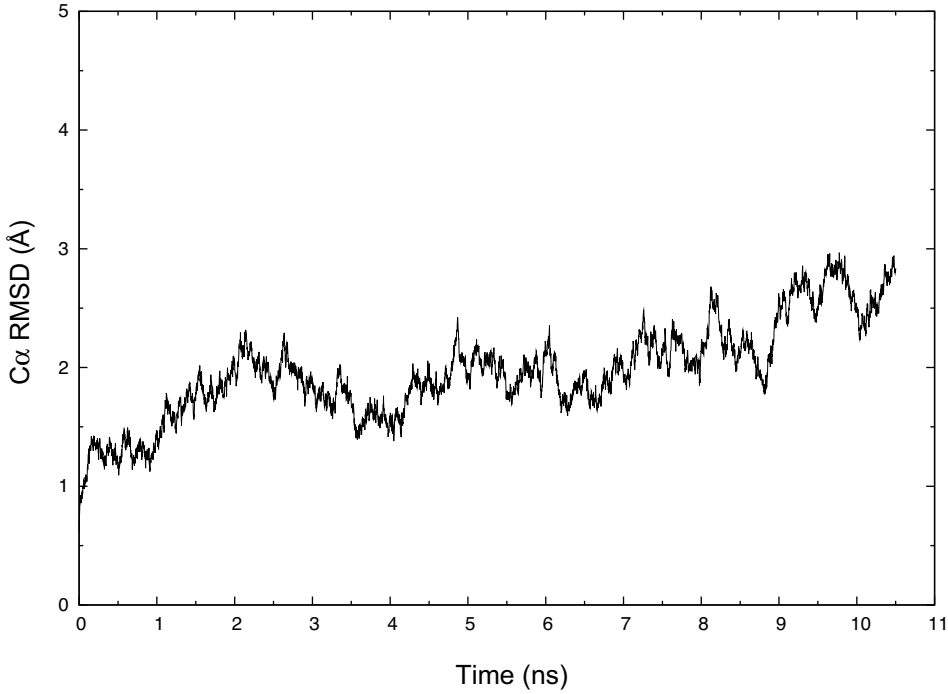

Fig. S1. A plot of the rmsd from the closed-form crystal structure (residues 5–251) against time during the 10.5-ns MD trajectory of the C465 simulation.

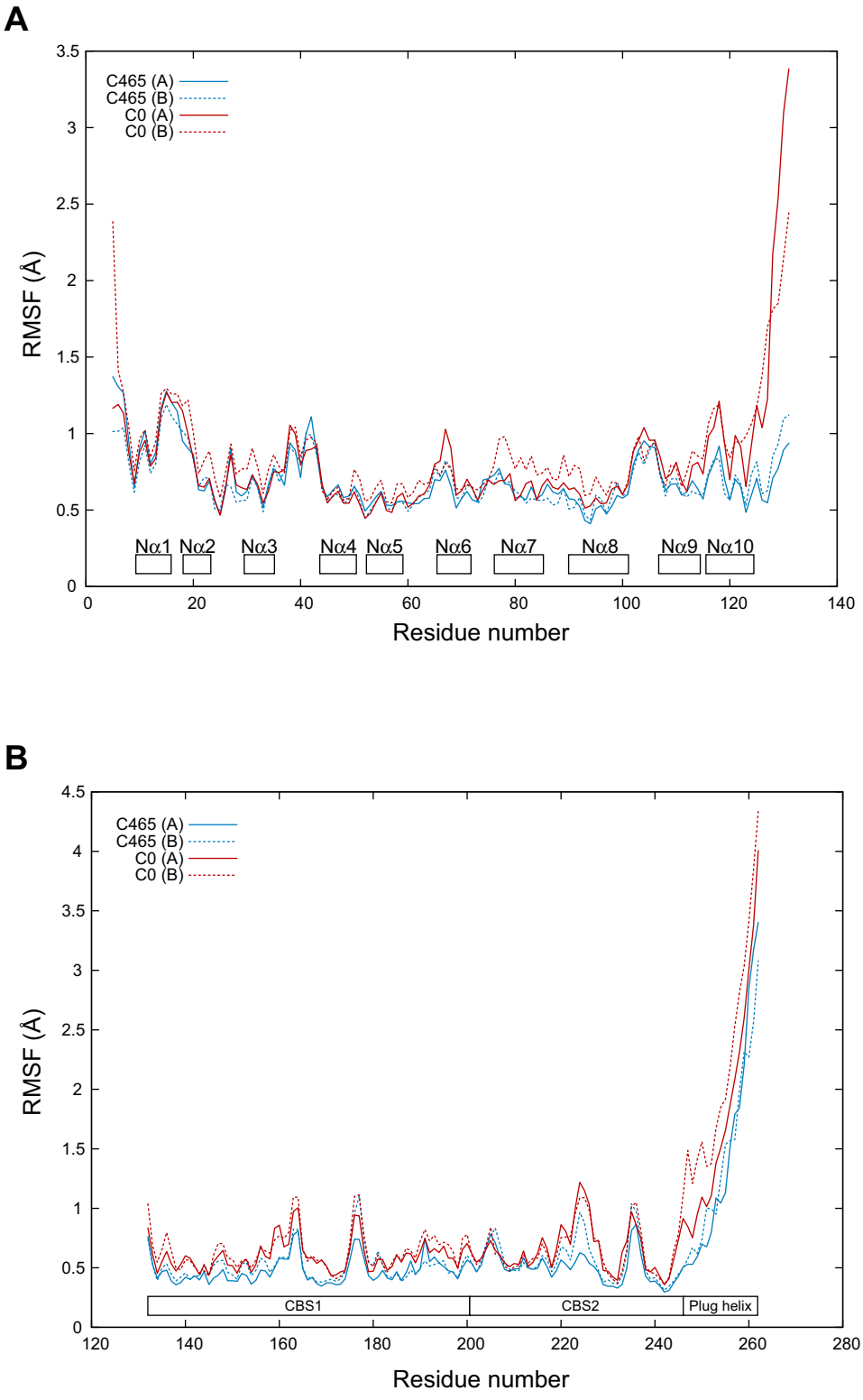

Fig. S2. Plots of rms fluctuations of each residue in the N (*A*) and CBS (*B*) domains from the average structures during the C465 and C0 simulations. The solid and dashed lines show the rms fluctuations of the A and B molecules of the dimer, respectively.

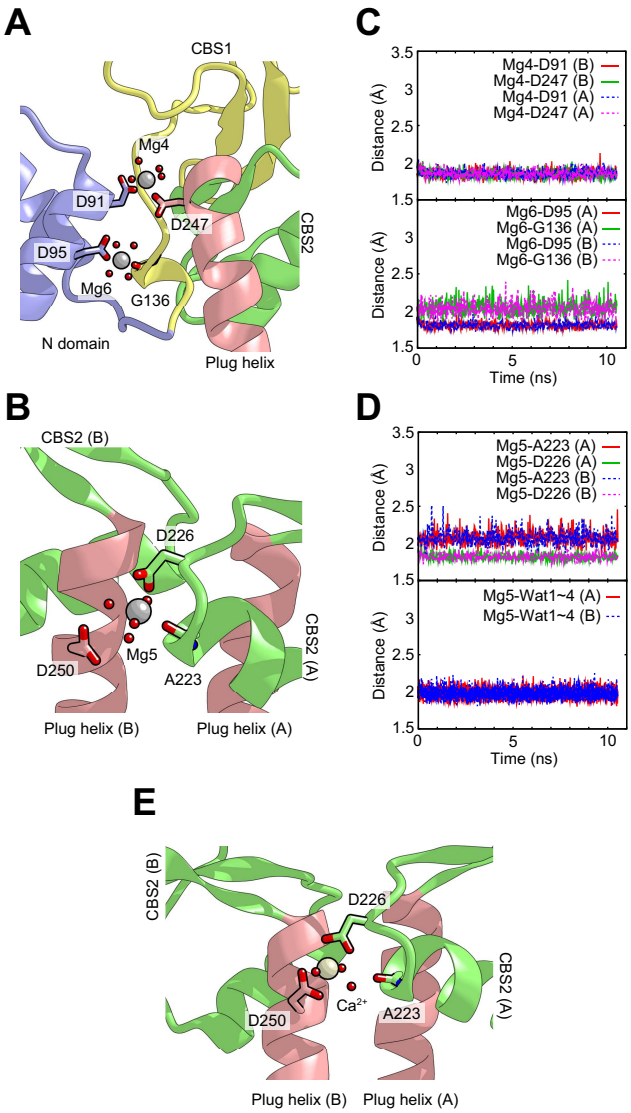

Fig. S3. Mg^{2+} and Ca^{2+} coordination manners of the MgtE cytosolic domains. (*A* and *B*) Coordination manners of Mg4 and Mg6 (*A*) and Mg5 (*B*) by MgtE at 10.5 ns of the C465 simulation. The protein backbones are depicted by ribbon models, with the same coloring scheme as Fig. 1. Mg^{2+} ions and coordinated water molecules are shown as gray and red spheres, respectively. The side chains involved in the Mg^{2+} binding are shown as stick models. (*C Upper*) The distances between Mg4 and its protein ligands (Oδ atoms of Asp-91 and Asp-247). (*C Lower*) The distances between Mg6 and its protein ligands (Oδ atom of Asp-95 and main-chain carbonyl oxygen of Gly-136). The distances for both of the subunits are shown. (*D Upper*) The distances between Mg5 and its protein ligands (Oδ atom of Asp-226 and main-chain carbonyl oxygen of Ala-223). (*D Lower*) The distances between Mg5 and water ligands. The distances for both of the subunits (subunit A and subunit B) are shown. (*E*) Coordination manner of Ca^{2+} by site 5 of the CBS domain at 10.0 ns of the Ca5 simulation.

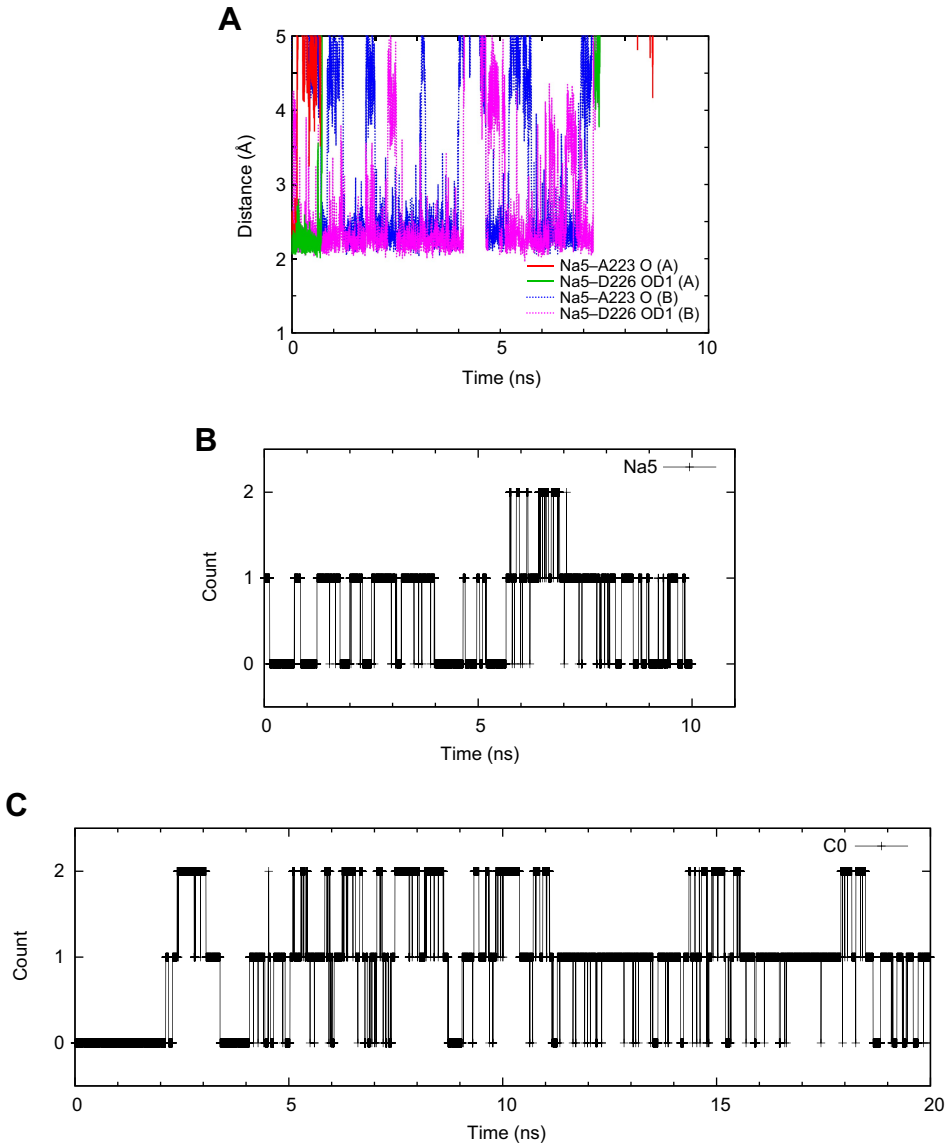

Fig. S4. The interactions between Na^+ and site 5. (*A*) Time series of distances between Na^+ and the closest oxygen atoms (main-chain O atoms of Ala-223 and side-chain carboxyl O atoms of Asp-226) in the Na5 simulation. The distances in each subunit (indicated by ''A'' and ''B'' in each panel) are separately plotted. (*B* and *C*) The occupancies of Na^+ at site 5 of the CBS domain against time in the simulations Na5 (*B*) and C0 (*C*). The occupancies were evaluated as follows. For all of the sodium ions, we measured three distances for the three oxygen atoms of the Mg^{2+} binding sites 5 (i.e., carbonyl oxygen of Ala-223 and two carboxyl oxygens of Asp-226), respectively. If one or more of these distances is <3 Å, we consider the site to be occupied by the sodium ion. Therefore, the occupancy has an integer value from 0 to 2, because the MgtE cytosolic domain contains two sites 5. In the Na5 simulation, one of the Na^+ placed at site 5 had already diffused after the equilibration phase, and thus the occupancy of the production run (*B*) started from 1.

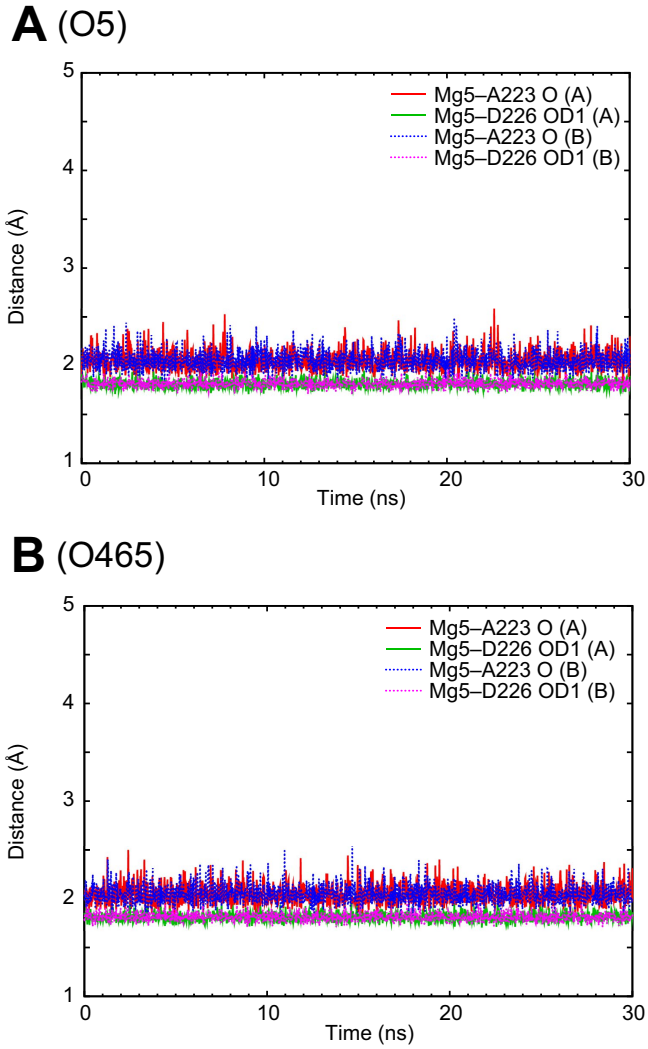

Fig. S5. Coordination manner of Mg^{2+} in the O5 and O465 simulations. Time series of distances between Mg^{2+} and the closest oxygen atoms (main-chain O atoms of Ala-223 and side-chain carboxyl O atoms of Asp-226) in the O5 (*A*) and O465 (*B*) simulations are plotted. The distances in each subunit (indicated by ''A'' and ''B'' in each panel) are separately plotted.

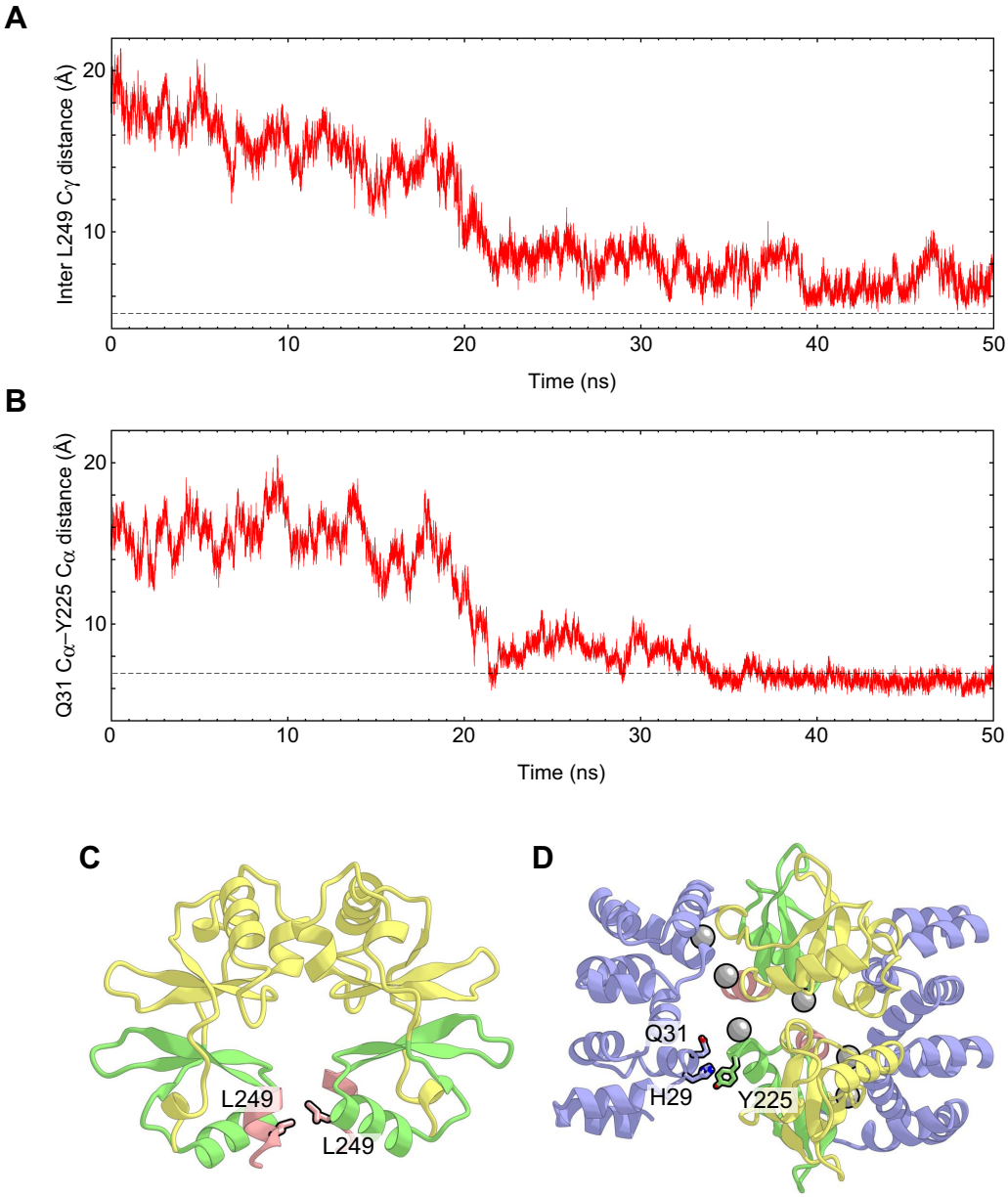

Fig. S6. Recovery of the native interactions observed in the simulation O465. (*A*) Time series of the distance between the Cγ atoms of Leu-249 of the two subunits. (*B*) Time series of the distance between the Cα atoms of Gln-31 and Tyr-225. (*C*) Interaction between His-29 and Gln-31 at the tip of the N domain and Tyr-225 in the CBS domain of the other subunit. The side chains of His-29, Gln-31, and Tyr-225 are shown in stick models, and the bound Mg^{2+} ions are depicted by balls (*D*). The protein main chain is shown in a ribbon model.

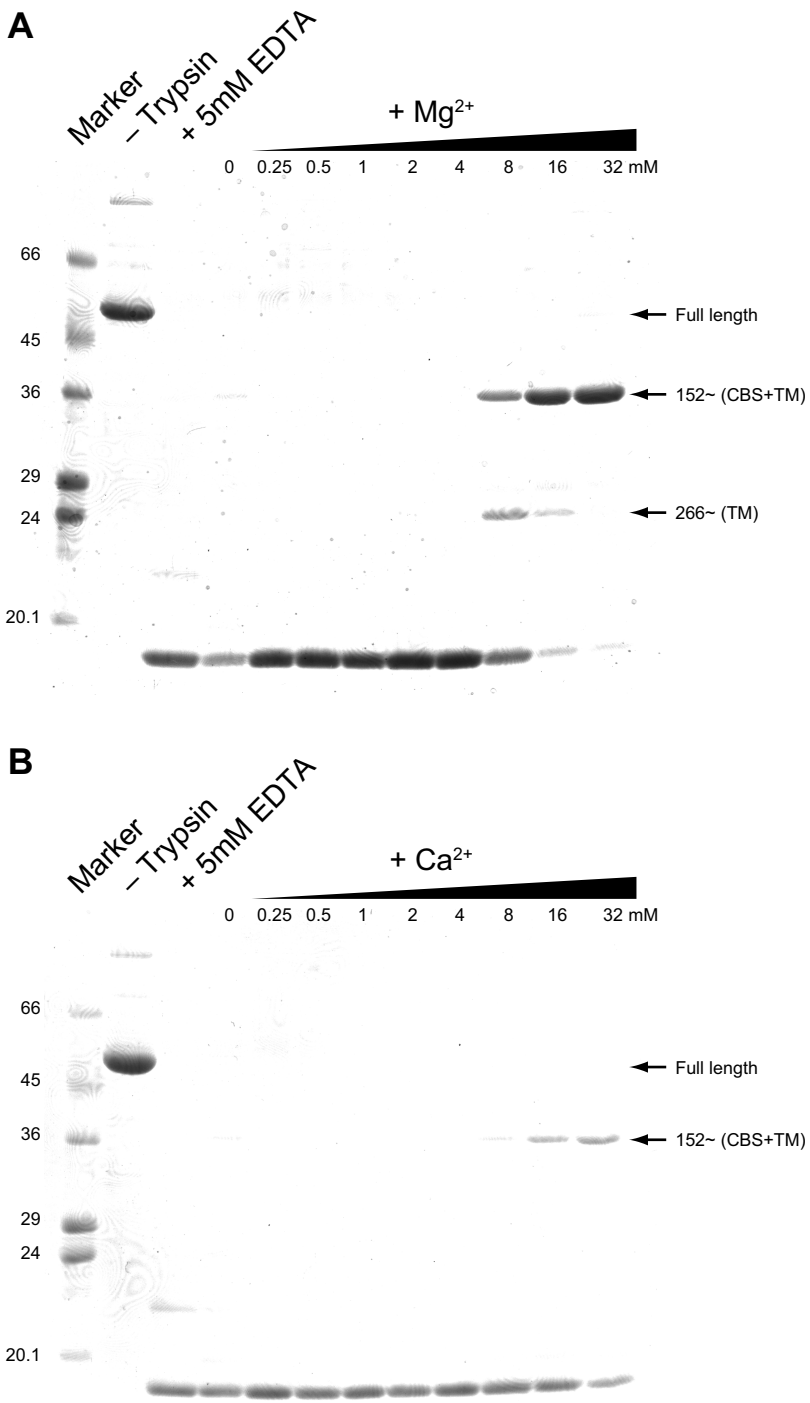

Fig. S7. Protease protection of the MgtE cytosolic domain by Mg^{2+} (*A*) and Ca^{2+} (*B*). The numbers with arrows on the right side indicate the starting residues of the fragments generated by proteolysis. The numbers on the left side indicate the molecular mass (in kilodaltons) of the marker.